Progress Estimation of an Excavation Pit

A. Vierling[1], T. Groll[1], D. Meckel[1], K. Heim[2], D. Walter[2], L. Scheidhauer[2], K. Körkemeyer[2] and K. Berns[1]

[1]Department of Computer Science, Robotics Research Lab, University of Kaiserslautern, Germany
[2]Department of Civil Engineering, Chair in Construction Management, University of Kaiserslautern, Germany

{vierling,groll,meckel,berns}@cs.uni-kl.de,
{kristina.heim,daniel.walter,lukas.scheidhauer,karsten.koerkemeyer}@bauing.uni-kl.de

Abstract -

This paper presents a method for automated excavation speed and progress estimation. First, a measure for the progress speed of an excavation pit is taken from the literature and evaluated regarding the possibility for automation. For each possible parameter, an automated extraction algorithm is presented. The used system is an autonomous excavator arm of a backhoe loader where the used hardware and software system is described. Experimental evaluation of the presented approach has been done with the autonomous system for a small trench, including multiple digging cycles. The resulting measurements seem to include some systematic errors which could be identified and suitable sanity checks could be implemented, removing the erroneous measurements. The remaining measurements were used to determine the excavation speed of the autonomous excavator arm and compared to the values of experienced and amateur operators.

Keywords -

Excavation; Progress Estimation; Autonomous System; Sensors

1 Introduction & Related Work

In recent years the demand in construction has increased tremendously, and presumably the trend will continue with an estimated growth of 3.5% per year till 2030 [1], where infrastructure construction is deemed as the most rapidly growing subsector with an estimated annual growth of 4% [1] till 2030. However, a major global problem in construction are delays. There exist a multitude of reasons for these delays, but [2] identified a "poor planning and scheduling" as one of the top 3 delay factors. In order to make it possible to react to such mishaps in planning and scheduling, it is necessary to be able to detect delays as early as possible. A continuous comparison between the planned and the real timeline would be needed, but it is not feasible to do such checks by hand. Therefore, these comparisons need to be automated. While the planning data is usually present in a suitable digital form, the real schedule is much more difficult to extract, and strongly depends on the exact construction task. A specific activity in nearly all construction sites is the excavation of a construction pit.

Figure 1. Excavator with additional sensor system (blue circle)

The volume estimation of such a construction pit is a well-researched problem from the theoretical point of view [3, 4, 5, 6]. However, estimation by real sensor data is not well researched, and if, then by using additional sensors in the surrounding of the pit [7] which might not be applicable for all construction sites. A more promising trend is the advancement in autonomous excavation, which inherently also mandates a pit monitoring. Here current research deals with the lower [8] and higher level [9] control, but also with the environment perception [10] and specifically the modeling of it [11, 12]. Combining the two levels has only recently become possible, as in [13], which uses similar sensors and representations, but does not specifically tackle the estimation of the excavation progress or speed. The paper at hand will also try to solve the problem of an automatic progress estimation utilizing autonomous excavation. An autonomous backhoe loader, more specifically the excavator's arm, is used for a prototypical implementation of an automated excavation state and speed monitoring. The used hardware and already existing software of the backhoe loader is described in section 2, and the methodology for extracting additional sensor data for a progress estimation is described in section 3. Afterwards and experimental evaluation is done in 4 and discussed in section 5.

2 System & Preliminary Work

The progress estimation of the excavation pit should be based on an autonomous excavation arm of a backhoe loader. Of course, such an autonomous system already yields a lot of helpful intermediate states and systems, which will be beneficial for the estimation, and are therefore described in this section.

2.1 Hardware

The used backhoe loader is a *John Deere 410J TMC* with a front-loader and an excavation arm, an image of the machine can be seen in figure 1. The backhoe loader is already equipped with encoders that give the position of each joint, as well as a control system to control each of the joints via CAN-bus signals. Additionally, a *Microstrain 3DM-GX5-25* Inertial Measurement Unit (IMU) and a *Hemisphere V320* global navigation satellite system (GNSS) is mounted on the top of the cabin, and a corresponding Real Time Kinematic (RTK) base station is placed in the vicinity and connected to the GNSS system. With this, a precise localization of the machine can be achieved. For the perception of the surroundings an *Ouster OS0-128* 3D-laser scanner with 128 lines and a Field-of-View of 90° × 360° and a *IFM O3D301* Time-of-Flight (ToF) camera is mounted next to a simple RGB-webcam on the crowd.

2.2 Software

The higher-level behavior-based control system for the excavation process is mainly based on the architecture already described in [14]. A short summary is given in figure 3. Essentially the complete digging cycle is divided into 4 phases, "move to digging", "digging", "move to dumping", and "dumping" arranged as a state machine. Each phase is further divided into smaller motion primitives. Transitions between phases happen when the right conditions, e.g., bucket angle, are met.

One preliminary perception algorithm which is used in this work is the bucket volume estimation described in [15]. Here, a ToF-camera measures a point cloud of the bucket. Then, a rasterized grid-map is created. Afterward, the difference to a grip-map of the empty bucket is calculated. This difference map allows the estimation of the filled volume inside the bucket. Also other estimation techniques [16] [17] for the bucket volume and fill level exist, but as the one in [15] was specifically implemented for the excavator at hand it was an obvious choice. Another used result is the classification of rocks inside a rock pile, described in detail in [18]. Here, an RGB-image and a depth-image is used to capture the scene. A wathershed-segmentation algorithm extracts pixels belonging to different rocks. With these pixel segmentations, an estimation of the rock sizes becomes feasible. In [18], this approach was used to determine if a rock would need to be crushed for loading, but here it will be used in a slightly different manner, as described later.

3 Approach & Implementation

As a next step, one needs to lay a foundation of how a suitable progress estimation of an excavation pit can be done. There are already methods known to parameterize the progress speed in civil engineering. The most obvious speed estimation would be to measure the excavated volume per time. However, one wants to normalize this excavation speed with respect to the current circumstances. This adapted speed is usually called *performance* $Q_n[\frac{m^3}{h}]$ and the relevant parameters will be explained further. Afterward, new methodologies on how to extract necessary information from the sensor data are given.

3.1 Progress Estimation

The main basis of the progress estimation is based on the works of Girmscheid, especially [19, 20]. An overview of the necessary parameters is given in table 1.

Name	Symbol	Unit	A/H
Nominal Bucket Volume	V_B	m^3	A
Cycle time	t_c	s	A
Dissolving factor	α	1	A
Fill factor	ϕ	1	A
Trench depth factor	f_1	1	A
Rotation angle factor	f_2	1	A
Emptying accuracy	f_3	1	H
Teeth condition	f_4	1	H
Maintenance	f_5	1	H
Operator	η_1	1	H
Operating condition	η_2	1	H
Machine utilization rate	η_G	1	H

Table 1. Progress estimation parameters according to [19, 20]. Names are translated, and symbols are adapted. Column A/H shows whether the parameter will be assumed to be measured automatically (A) or by hand (H).

The performance can then be computed as:
$Q_n = \frac{V_B}{t_c} \times 3600 \times \alpha \times \phi \times f_1 \times f_2 \times f_3 \times f_4 \times f_5 \times \eta_1 \times \eta_2 \times \eta_G$
From the needed parameters, the ones that can be measured

Figure 2. Image of the start of the four different digging phases of the excavation process, from left to right: "Digging", "Move to Dumping", "Dumping", "Move to Digging"

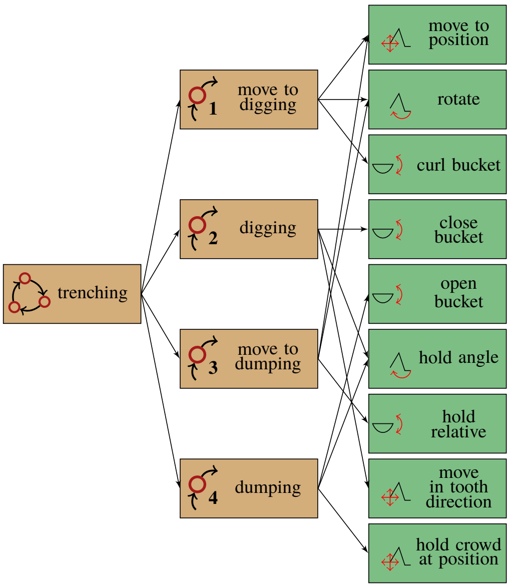

Figure 3. The architecture of the trenching process [14]. Images of each phase can be seen in figure 2

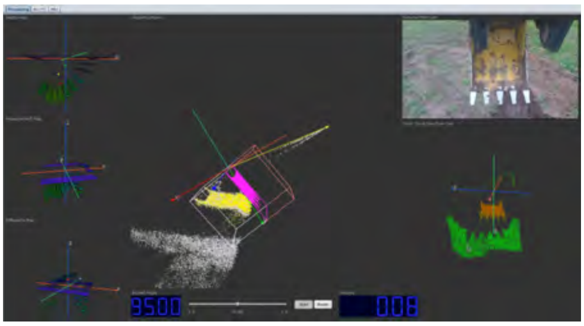

Figure 4. Bucket fill level estimation [15]

automatically are described first. The datasheet of the machine defines the nominal bucket volume. The cycle time is the time between the start and end of each digging cycle. The dissolving factor is the ratio between the volume of the compacted and the loosened soil. The fill factor measures how much of the fill level of the bucket really corresponds to the volume of the content, e.g., for big rocks, a lot of space is unused compared to fine sand. The trench depth describes the depth of the current digging cycle. The rotation angle is defined as the angle between the digging and dumping positions in each cycle. All other given parameters can currently not be determined automatically. Some are also not relevant for autonomous excavation and can not be calculated in such an excavator. This includes the emptying accuracy, the size of the dumping region (which is always a "point" in our autonomous excavation scenario), as well as the operator factor (skill factor). Similarly, the conditions of the teeth and the maintenance state can be more easily extracted from external sources. In principle it is possible to estimate both with additional sensors, e.g. the teeth state could be estimated by using the point cloud of the time-of-flight camera and then estimating how sharp the teeth still are. However, in both cases extracting information about the working hours form the software of the manufacturer seems to be the better solution, as this is usually recorded and often accessible to the user. However, an integration is machine and manufacturer specific and therefore omitted here. The operating conditions are not as clearly defined and include the effect of weather, as well as the quality of preparation work and are therefore not measured automatically.

3.2 Data Abstraction

In order to extract the defined parameters, additional evaluation of the sensor and control data has to be done, which is not present in the preliminary work. A valuable help is here the knowledge which action is currently executed by the excavator's arm. The visualization of each phase or action can be seen in figure 2. With this information, the cycle time can be directly calculated by saving the timestamp of the start of the "digging"-phase and calculating the difference till the subsequent "digging"-phase starts. Similarly, the trench depth can be deduced by the z-position of the bucket teeth, which can be calculated by the kinematic model as in [14], at the start of the "move to dumping" position, e.g., the end of the "digging"-phase plus an offset accounting for the bucket width. In the same manner, the rotation angle can be computed by taking the difference of the yaw-values at the start of the "dumping" and "digging" phases.

The fill and dissolving factors are not as easily calculated. For the fill factor, the RGB-image and depth image at the start of the "digging"-phase is considered, and then a classification of the visible rock sizes, as in [18], is used. The fill factor is then determined according to the rock size in the image and the table 2.

Rock Size (s)	Fill Factor
$s < 63mm$	1
$63mm \leq s < 200mm$	0.85
$200mm \leq s$	0.75

Table 2. Adapted fill factors. In [19, 20] fill factors for all soil classes (defined by [21]) are given, but the fill factors do not differ much. The used adaptions are a compromise between classification difficulty and effectiveness

In order to calculate the dissolving factor, the estimation of the bucket fill level as in [15] is used, which corresponds to the volume of the loosened soil. To calculate the volume of the compacted soil, the 3D point cloud of the laser scanner is used. The point cloud is rasterized into a grid map, as seen in figure 6. Between the start of two "digging"-phases, the height difference of the grid-cells belonging to the target map, which defines the wanted final form of the pit, are calculated. The compacted volume can be estimated with this depth difference and the grid size. A major disturbance in this method is the soil, which is only moved by the bucket and not loaded into it. Therefore one would like to include all grid-cells in the difference calculation, but this leads to another problem. Figure 6 shows the laser scanner-based pose estimation. The measured points of each scan are fused into the map. Although the terrain around the excavator is flat, the grid map shows increasing terrain further away from the excavator. While the accuracy of the laser scanner reduces with distance, the divergences are mainly due to the fact that the exact pose of the scanner is not known because of the vibrations of the excavator's arm. The pose further deteriorates during the digging process. This pose error is amplified by the distance, which is why it is not directly visible in the vicinity of the excavator but still plays a role in the measurements. Therefore not all grid-cells should be chosen. As a trade-off the cells directly neighboring the target map are additionally used for the difference calculation.

4 Experiments

For the experimental evaluation, a trench with dimensions $2m \times 1m \times 5m$ (Height×Width×Length) has been excavated. An image of the excavated trench can be seen in figure 5. The resulting values can be seen in table 3. In

Figure 5. Final excavated trench

the area of the experiments no bigger rocks were present. Therefore the fill factor was always assumed to be 1 and is excluded from the table.

Some cycles in table 3 include clear measurement errors. For instance, the GPS Signal was lost in cycles 6 and 18. Therefore, the depth offset of the backhoe's position is wrong. For other cycles, e.g., 6 and 19, the estimated compacted volume is bigger than the loosened volume. This can only happen for large rocks. In general, an overestimation of the compacted volume seems to be a trend. This is probably due to the way the autonomous excavation happens: the excavator's arm often goes too deep into the ground and pulls much more soil out of the ground than can fit in the bucket. This soil will be measured as removed from the pit, but not as loosened volume in the bucket. However, this error should be leveled out, when this soil is scooped up and moved to the correct dumping position. In order to have a reasonable speed estimation at all times, a sanity check taking these two problems into account is proposed. It includes the following rules:

- Skip measurement if $f_1 > 4.9m$ (maximum digging depth)
- Skip measurement if $\alpha > 1$ and $\phi > 1$ (Reminder: $\phi = 1$ in all provided experiments)

If only the remaining measurements are included, the estimated performance Q_n is resulting in 60% of a proficient excavator operator. In comparison, an amateur would achieve roughly 65% according to [19, 20], which suggests that the measurement methods yield suitable results.

5 Conclusion

The presented approach for the estimation of the excavation speed seems to be promising, as it yields good results in many cases. Even though some measurement errors are present, they do not affect the task's suitability. Still, general improvements in the estimation of the loosened soil could be done. Possible extensions include adapting the size of the grid-cells as well as a more precise localization

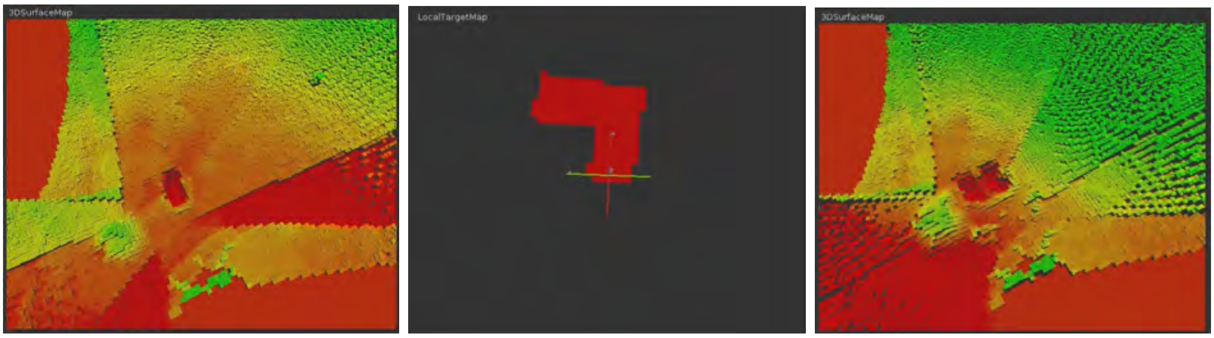

Figure 6. Grid map of two consecutive digging cycles (left and right) and corresponding target map (middle). The cell heights are color-coded. Green indicates a high positive value and red a high negative value. The pit can be seen as dark red cells in the middle of the grid maps

of the laser scanner to achieve a better fusion. Approaches like scene flow or ICP-matching seem suitable for improving this aspect. This would also reduce the effect of a lost GPS signal which is a major disturbance in the current implementation. However, in general, with the advancement of the automation of construction machinery and an increasing number of sensors on a construction site, similar approaches are promising. A detailed picture of the state of the complete construction site could be achieved by combining the knowledge of different vehicles.

6 Acknowledgments

The implementation, methodology and evaluation of this paper were partially funded by the German Federal Ministry of Transport and Digital Infrastructure (Bundesministerium für Verkehr und digitale Infrastruktur **BMVI**) per the *Infra-Bau 4.0* project.

References

[1] Graeme Harrison and Jeremy Leonard. Future of construction. Technical report, Oxford Economics, September 2021. URL `https://www.oxfordeconomics.com/recent-releases/Future-of-Construction`.

[2] Youcef J.-T. Zidane and Bjorn Andersen. The top 10 universal delay factors in construction projects. *International Journal of Managing Projects in Business*, 11(3):650–672, Jan 2018. ISSN 1753-8378. doi:10.1108/IJMPB-05-2017-0052. URL `https://doi.org/10.1108/IJMPB-05-2017-0052`.

[3] Chun-Sung Chen and Hung-Cheng Lin. Estimating pit‐excavation volume using cubic spline volume formula. *Journal of Surveying Engineering*, 117(2):51–66, 1991. doi:10.1061/(ASCE)0733-9453(1991)117:2(51). URL `https://ascelibrary.org/doi/abs/10.1061/%28ASCE%290733-9453%281991%29117%3A2%2851%29`.

[4] B. Mukherji. Estimating 3d volume using finite elements for pit excavation. *Journal of Surveying Engineering*, 138(2):85–91, 2012. doi:10.1061/(ASCE)SU.1943-5428.0000059. URL `https://ascelibrary.org/doi/abs/10.1061/%28ASCE%29SU.1943-5428.0000059`.

[5] Ragab Khalil. Credibility of 3d volume computation using gis for pit excavation and roadway constructions. *American Journal of Engineering and Applied Sciences*, 8:434–442, 04 2015. doi:10.3844/ajeassp.2015.434.442.

[6] Maxim Tyulenev, O. Litvin, M. Cehlár, Sergey Zhironkin, and M. Gasanov. Estimation of hydraulic backhoes productivity for overburden removing at kuzbass open pits. *Acta Montanistica Slovaca*, 22: 296–302, 01 2017.

[7] Maximilian Bügler, Gbolabo Ongunmakin, Jochen Teizer, Patricio Vela, and Andre Borrmann. A comprehensive methodology for vision-based progress and activity estimation of excavation processes for productivity assessment. 01 2014. doi:10.13140/RG.2.1.4630.2561.

[8] Guilherme J. Maeda, David C. Rye, and Surya P. N. Singh. Iterative autonomous excavation. In Kazuya Yoshida and Satoshi Tadokoro, editors, *Field and Service Robotics: Results of the 8th International Conference*, pages 369–382, Berlin, Heidelberg, 2014. Springer Berlin Heidelberg. ISBN: 978-3-642-40685-0, DOI: https://doi.org/10.1007/978-3-642-40686-7_25.

Cycle	t_c [s]	Compacted Volume [m^3]	Loosened Volume [m^3]	α [1]	f_1 [1]	f_2 [1]
01	72,8911	0,2389	0,3385	0,7057	0,2606	62,6429
02	72,9800	0,2929	0,3471	0,8440	0,2269	61,1909
03	66,8381	0,6701	0,3590	1,8666	0,6320	61,4380
04	186,7704	0,3922	0,2905	1,3501	0,7886	62,5649
05	194,0915	0,1275	0,2709	0,4709	0,6929	61,1918
06	690,1479	2,1733	0,2675	8,1247	56,9951	61,2457
07	65,0554	0,0750	0,2419	0,3102	1,1417	61,1202
08	72,5589	0,3927	0,2743	1,4316	1,2213	62,8282
09	370,7839	0,5742	0,3167	1,8129	1,2758	62,3137
10	67,6435	0,0653	0,2808	0,2325	1,3913	61,2390
11	65,2036	0,0733	0,1967	0,3726	1,0822	62,4411
12	139,5601	0,3869	0,1954	1,9805	1,5954	62,2147
13	248,4500	0,5289	0,1807	2,9280	0,9151	60,9772
14	179,0602	0,0992	0,1807	0,5491	0,7188	62,9664
15	85,5514	0,7926	0,2308	3,4334	0,5826	62,8606
16	68,8132	0,4620	0,2484	1,8601	1,4567	62,1681
17	120,2028	0,3718	0,2195	1,6937	0,4379	61,7577
18	1745,1303	0,8514	0,1395	6,1015	123,8112	63,1761
19	54,9628	2,3939	0,2204	10,8624	0,4236	62,5417
20	60,4940	0,5597	0,2977	1,8800	0,3359	62,3002
21	56,5907	0,5973	0,2339	2,5540	0,2400	62,8761

Table 3. Experimental evaluation

[9] Daniel Schmidt. *Shaping the Future - A Control Architecture for Autonomous Landscaping with an Excavator*. RRLab Dissertations. Verlag Dr. Hut, München, 2016. `http://www.dr.hut-verlag.de/978-3-8439-2816-8.html` ISBN-13: 978-3-8439-2816-8.

[10] Thomas Emter, Christian Frese, Angelika Zube, and Janko Petereit. Algorithm Toolbox for Autonomous Mobile Robotic Systems. *ATZoffhighway worldwide*, 10(3):48–53, sep 2017.

[11] Philipp Woock, Nina F. Heide, and Daniel Kuehn. Robotersysteme für die dekontamination in menschenfeindlichen umgebungen. In *Proceeding at Leipziger Deponiefachtagung 2020. Leipziger Deponiefachtagung (LDFT-2020), March 3-4, Leipzig, Germany*. n.n., 2020.

[12] Nina Felicitas Heide, Philipp Woock, Maximilian Sauer, Timo Leitritz, and Michael Heizmann. Ucsr: Registration and fusion of cross-source 2d and 3d sensor data in unstructured environments. In *IEEE 23rd International Conference on Information Fusion (FUSION)*, 2020.

[13] Dominic Jud, Simon Kerscher, Martin Wermelinger, Edo Jelavic, Pascal Egli, Philipp Leemann, Gabriel Hottiger, and Marco Hutter. Heap - the autonomous walking excavator. *Automation in Construction*, 129: 103783, 2021.

[14] Tobias Groll, Steffen Hemer, Thorsten Ropertz, and Karsten Berns. A behavior-based architecture for excavation tasks. In *34th International Symposium on Automation and Robotics in Construction (ISARC)*, pages 1005–1012. International Association for Automation and Robotics in Construction, June 28-July 1 2017. DOI: https://doi.org/10.22260/ISARC2017/0139.

[15] Steffen Hemer, Tobias Groll, and Karsten Berns. Backhoe bucket volume and trench monitoring using a time-of-flight camera. In *7. Fachtagung Baumaschinentechnik 2018: Digitalisierung, Automatisierung, Mensch*, Dresden, September 20–21 2018. Forschungsvereinigung Bau- und Baustoffmaschinen e.V. FVB, Forschungsvereinigung Bau- und Baustoffmaschinen e.V. FVB.

[16] Liangjun Zhang, Jinxin Zhao, Pinxin Long, Liyang Wang, Lingfeng Qian, Feixiang Lu, Xibin Song, and Dinesh Manocha. An autonomous excavator system for material loading tasks. *Science Robotics*, 6(55): eabc3164, 2021. doi:10.1126/scirobotics.abc3164. URL `https://www.science.org/doi/abs/10.1126/scirobotics.abc3164`.

[17] Haodong Ding, Xibin Song, Zhenpeng He, and

Liangjun Zhang. Real-time volume estimation of mass in excavator bucket with lidar data. In Chen Feng, Thomas Linner, Ioannis Brilakis, Daniel Castro, Po-Han Chen, Yong Cho, Jing Du, Semiha Ergan, Borja Garcia de Soto, Jozef Gasparík, Firas Habbal, Amin Hammad, Kepa Iturralde, Thomas Bock, Soonwook Kwon, Zoubeir Lafhaj, Nan Li, Ci-Jyun Liang, Bharadwaj Mantha, Ming Shan Ng, Daniel Hall, Mi Pan, Wei Pan, Farzad Rahimian, Benny Raphael, Anoop Sattineni, Christian Schlette, Isaac Shabtai, Xuesong Shen, Pingbo Tang, Jochen Teizer, Yelda Turkan, Enrique Valero, and Zhenhua Zhu, editors, *Proceedings of the 38th International Symposium on Automation and Robotics in Construction (ISARC)*, pages 696–703, Dubai, UAE, November 2021. International Association for Automation and Robotics in Construction (IAARC). ISBN 978-952-69524-1-3. doi:10.22260/ISARC2021/0094.

[18] Tobias Groll, Steffen Hemer, and Karsten Berns. Classification of rocks inside a rock pile for task planning. In *8. Fachtagung Baumaschinentechnik 2020: Maschinen, Prozesse, Vernetzung*, 2020.

[19] Gerhard Girmscheid. *Leistung im Baubetrieb*, pages 1–18. Springer Berlin Heidelberg, Berlin, Heidelberg, 2010. ISBN 978-3-642-13795-2. doi:10.1007/978-3-642-13795-2_1. URL `https://doi.org/10.1007/978-3-642-13795-2_1`.

[20] Gerhard Girmscheid. *Faktoren*, pages 249–279. Springer Berlin Heidelberg, Berlin, Heidelberg, 2010. ISBN 978-3-642-13795-2. doi:10.1007/978-3-642-13795-2_8. URL `https://doi.org/10.1007/978-3-642-13795-2_8`.

[21] DIN 18300. VOB - Vergabe- und Vertragsordnung für Bauleistungen - Teil C: Allgemeine Technische Vertragsbedingungen für Bauleistungen (ATV) - Erdarbeiten, September 2018.